Hindawi
Journal of Nanomaterials
Volume 2022, Article ID 9745418, 13 pages
https://doi.org/10.1155/2022/9745418

Research Article

Synthesis of AA8050/B_4C/TiB_2 Hybrid Nanocomposites and Evaluation of Computer-Aided Machining Parameters

T. Sathish,[1] Mohanavel Vinayagam,[2,3] T. Raja,[4] A. H. Seikh,[5] M. H. Siddique,[6] Ram Subbiah,[7] and Beruk Hailu[8]

[1]*Department of Mechanical Engineering, Saveetha School of Engineering, SIMATS, Chennai, 602 105 Tamil Nadu, India*
[2]*Centre for Materials Engineering and Regenerative Medicine, Bharath Institute of Higher Education and Research, Chennai, 600073 Tamil Nadu, India*
[3]*Department of Mechanical Engineering, Chandigarh University, Mohali-140413, Punjab, India*
[4]*Department of Mechanical Engineering, Vel Tech Rangarajan Dr. Sagunthala R&D Institute of Science and Technology, Chennai, Tamil Nadu, India*
[5]*Mechanical Engineering Department, College of Engineering, King Saud University, P.O. Box 800 Al-Riyadh 11421, Saudi Arabia*
[6]*Intelligent Construction Automation Centre, Kyungpook National University, Daegu, Republic of Korea*
[7]*Department of Mechanical Engineering, Gokaraju Rangaraju Institute of Engineering & Technology, Hyderabad, Telangana 500090, India*
[8]*Faculty of Mechanical Engineering, Haramaya Institute of Technology, Haramaya University, Ethiopia*

Correspondence should be addressed to Beruk Hailu; beruk.hailu@haramaya.edu.et

Received 8 May 2022; Accepted 1 August 2022; Published 31 August 2022

Academic Editor: Arpita Roy

This research focusses on synthesizing the hybrid nanocomposite samples with AA8050 and the reinforcement of B_4C and TiB_2 nanoparticles at 3 different quality grades. To investigate their machinabilities on the prepared composites in the computer-aided machining centre, the objectives are maximizing the material removal rate (MRR) and minimizing the surface roughness for a specific application. Stir casting process was employed in synthesizing the hybrid nanocomposite samples. Utilizing CNC turning centre was employed to investigate machinability performance on hybrid nanocomposite samples. The PVD-coated HSS tool and dry cutting environment were considered. The quality of machining was investigated by observing the surface roughness on the machined surfaces of samples of hybrid nanocomposite. The machining rate was investigated through the response of material removal rate at as per Taguchi design of experiments L27 orthogonal array. The hybrid nanocomposite synthesizing parameter of contribution of nanoparticle reinforcement (8%, 10%, and 12%) and the Turing parameters include spindle speed (800 rpm, 1000 rpm, and 1200 rpm), machining feed (0.05 mm/rev, 0.10 mm/rev, and 0.15 mm/rev) and depth of cut (0.5 mm, 0.75 mm, and 1 mm). The best performing input levels were identified through Taguchi analysis and the involved input variables were analysed and prediction model developed through ANOVA. The maximum material removal rate and the minimum surface roughness were reordered as 1380 mm^3/min.

1. Introduction

Hybrid composites presented the high strength of the aluminium alloy for using reinforced particles. In the statistical analysis, the influence of higher cutting speed reduces the cutting force of the tool material. Results between the experimental work and the predicted values of the SiCp/Al nanocomposites, the cutting force is slightly reduced in the experimental work [1]. Using of carbide cutting tool for turning of E250 steel in the CNC turning process, the material removal rate is increased moderately. Optimum values are attained as 1100 rpm of spindle speed, 0.44 mm of depth of cut, and 0.2 mm/min of feed rate. These optimal output parameters provided better surface finish as well as high MRR [2]. In automobiles, wheel axles are made on hardened alloy steels for giving high strength and absorption of shocks

Table 1: Chemical composition of AA8050.

Material	% of composition
Cr	0.05
Cu	0.05
Fe	1.3
Mg	0.05
Mn	0.80
Si	0.03
Zn	0.1
Al	Remaining

Figure 1: Schematic view of stir casting process equipment.

and vibrations. Different parameters such as cutting speed, machining feed, depth of cut, relief angle nose radius, and type of insert are involved in machining of hardened alloy steels. The L18 orthogonal array (OA) is suitable to examine the surface roughness and machinability characteristics of the hardened alloy steels. In this study, the influence of optimal parameters is reducing the tool flank wear such as 53.85%; similarly, the surface roughness also reduced by 15.95%. Optimal flank wear was obtained as 0.057 mm, and the optimum surface roughness value was attained as 1.0248 mm [3]. All the industries like as automotive, aerospace, marine, and structural components the 316L stainless steel was highly influenced. In machining of these materials, the tool has to be highly wear and the tool life also reduced increasing of tool life by the way of applying of lubrication with coolant. Using of coolant, the wear has to be approximately 9%. Dry machining increases the wear of the tool comparing to the coolant applied machining process [4]. Machining of titanium alloys is a difficult one; to overcome this, alternative machining techniques were applied. The tool wear was estimated under the working nature such as dry, wet, and cryogenic surroundings. Comparing the wet and dry nature machining, the cryogenic nature offered higher tool life such as 200% to others. Similarly, the surface roughness was reduced 71% by using cryogenic application. Comparing other methods such as wet and dry offered 64% of reduced surface roughness [5]. Aluminium alloy with reinforcement of silicon carbide nanoparticles is prepared by the stir casting route. Various parameters influencing the CNC turning process decided the surface finish and the MRR. This work concluded the 40 m/min of spindle speed, 0.100 mm/rev of feed rate, 0.3 mm of depth of cut, and 3% SiC, 7% Gr were recorded as optimal parameters [6]. The tungsten carbide inserts are effectively used in the CNC turning process; aluminium alloy (LM6) with silicon carbide particles reinforced composites are machined successfully. They [7] focused to reduce the cutting temperature, vibration, and surface roughness with different optimal parameters. The authors found the poor surface finish was attained due to composite particles sticking to the tool inserts. Many researchers intend to study the aluminium alloy metal matrix composites using coated tool material in the CNC turning process. Only few of the attempts are made on titanium alloy. This work was carried out on titanium metal matrix composites using carbide as well as cubic boron carbide inserts. Machinability study of surface roughness, cylindricity, cutting forces, and tool wear are carried out. In addition, the statistical analysis was included to evaluate the best parameter among the chosen parameters. CBN tool inserts offered good surface finish even in different spindle speeds [8–10]. This article discusses the synthesis of novel aluminium metal matrix composite with composite matrix of AA8050 with equal and hybrid reinforcement of B_4C nanoparticles and TiB_2 nanoparticles at various wt.% and investigates their machinability performance on CNC turning centre. The Taguchi design of experiments and analysis was preferred to optimize the machining parameters for maximizing material removal rate (MRR) and minimizing surface roughness on machined surfaces. With the best of our knowledge, such novel composites were not published or patented so far.

2. Experimental Details

2.1. Materials and Methods. This study conducts the machining process in the CNC turning centre using the material aluminium alloy with reinforcement of boron carbide (B_4C) nanoparticles and titanium diboride (TiB_2) nanoparticles. AA8050 aluminium alloy possesses high strength and excellent mechanical properties; adding of reinforcement nanoparticles, its strength is upgraded in a great level [11–14]. Automotive parts, aerospace components are to be made by using this material. High-strength nanoparticles of boron carbide and titanium diboride nanoparticles are used as reinforcement agent of this study. Boron carbide is a high hard material for antagonism against wear as well as a lightweight material [15]. Titanium diboride is an extreme heat conductivity material and also prevents oxidation, with good stability. The chemical composition of aluminium alloy 8050 is illustrated in Table 1.

Material preparation is conducted through stir casting process; the particles were reinforced at the time of stir casting [16–18]. Stir casted materials are machined through CNC turning using Diamond-Like Carbon- (DLC-) coated tungsten carbide tool [19–21]. CNC turning process is achieved by using different parameters applying L_{27} orthogonal array (Taguchi route). The outcome of this

Figure 2: Hybrid nanocomposite machinability investigated at CNC turning centre.

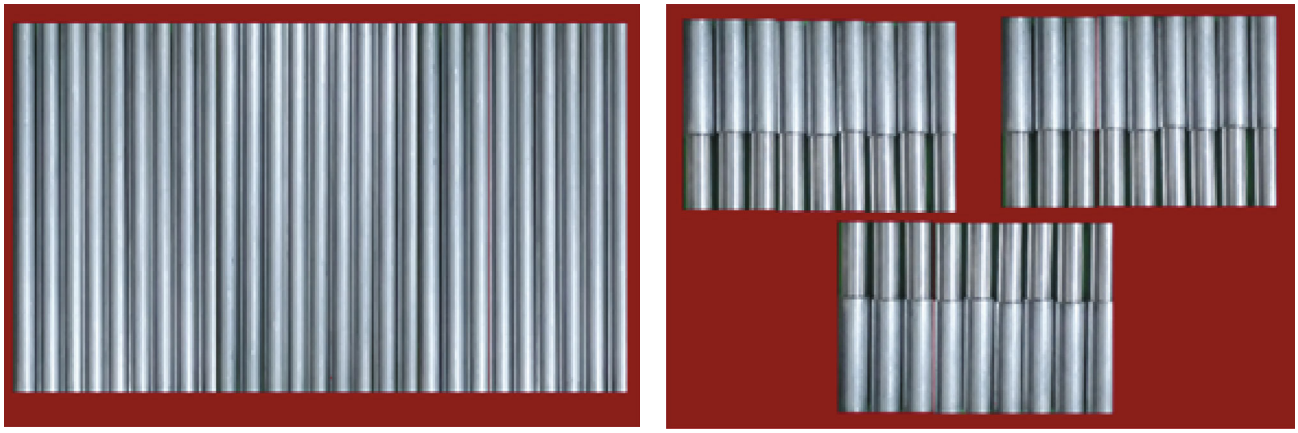

(a) (b)

Figure 3: Turning specimen: (a) hybrid nanocomposite before turning and (b) after turning.

Table 2: Parameters and their levels of MRR.

Level	Nanoparticle reinforcement (NS) (%)	Spindle speed (SS) (rpm)	Machining speed (MS) (mm/rev)	Depth of cut (DC) (mm)
1	8	800	0.05	0.50
2	10	1000	0.10	0.75
3	12	1200	0.15	1.00

experimental work is considered as surface roughness and material removal rate [22–24].

2.2. Experimental Procedure. Stir casting process is employed to this research work to produce the hybrid nanocomposite in the form of round rod. In stir casting process, the base material of aluminium alloy (AA8050) and the reinforced nanoparticles of boron carbide and nanoparticles of titanium diboride are mixed well [25–27]. The reinforced material is added to the base material at different weight percentages such as 8%, 10%, and 12%. Stir casting process is carried out using different parameters for producing the effective hybrid nanocomposite [28–30]. Stirring speed of 650 rpm, stirring time of 30 min, and stirring temperature of 900°C are used as parameters of the stir casting process [31]. The stir casting equipment is model SWAM EQUIP bottom pouring type stir casting as shown in Figure 1.

All the samples are machined using CNC turning machine (brand: Ace Micromatic; model: Super Jobber 500-LM CNC Lathe Machine). This machine was used to turn a maximum of 320 mm diameter and maximum of 500 mm length as shown in Figure 2. Diamond-Like Carbon- (DLC-) coated tungsten carbide tool is used for turning hybrid composite materials [32–34].

In the turning process, the different parameters and levels are used such as spindle speed (800 rpm, 1000 rpm,

Table 3: Summary of machining parameters and MRR.

Exp. runs	Nanoparticle reinforcement (%)	Spindle speed (rpm)	Machining feed (mm/rev)	Depth of cut (mm)	MRR (mm^3/min)
1	8	800	0.05	0.50	360
2	8	800	0.05	0.50	480
3	8	800	0.05	0.50	845
4	8	1000	0.10	0.75	736
5	8	1000	0.10	0.75	1180
6	8	1000	0.10	0.75	638
7	8	1200	0.15	1.00	1315
8	8	1200	0.15	1.00	1289
9	8	1200	0.15	1.00	578
10	10	800	0.10	1.00	481
11	10	800	0.10	1.00	394
12	10	800	0.10	1.00	617
13	10	1000	0.15	0.50	883
14	10	1000	0.15	0.50	1023
15	10	1000	0.15	0.50	1380
16	10	1200	0.05	0.75	1265
17	10	1200	0.05	0.75	595
18	10	1200	0.05	0.75	439
19	12	800	0.15	0.75	762
20	12	800	0.15	0.75	827
21	12	800	0.15	0.75	398
22	12	1000	0.05	1.00	986
23	12	1000	0.05	1.00	1128
24	12	1000	0.05	1.00	1264
25	12	1200	0.10	0.50	1018
26	12	1200	0.10	0.50	912
27	12	1200	0.10	0.50	650

and 1200 rpm), machining feed (0.05 mm/rev, 0.10 mm/rev, and 0.15 mm/rev), and depth of cut (0.5 mm, 0.75 mm, and 1 mm). All these parameters are effectively utilized, and turning operation was successfully carried out; each experimental trial run shows different output results such as MRR and result of surface roughness [35–37]. Figure 3 presents the AA8050/B_4C/TiB_2 of the hybrid nanocomposite material samples before and after machining.

Material removal rate was calculated by the volume of material removal from the specimen with specified time period [38]. The surface roughness was checked using a Mitutoyo tester (model: SJ210 Surface Roughness Tester). Surface roughness was estimated through conducting of three trials for each sample and averaging it [39]. Table 2 presents the parameters and their levels of MRR.

3. Results and Discussion

3.1. MRR. Table 3 represents all parameter correlation and the output result of material removal rate in a detailed manner. Maximum material removal rate of 1380 mm^3/min was obtained by 10% of nanoparticle reinforcement, 1000 rpm of spindle speed, 0.15 mm/rev of machining speed, and 0.50 mm of depth of cut [40].

Table 4: Response table for means (MRR).

Level	Nanoparticle reinforcement (%)	Spindle speed (rpm)	Machining speed (mm/rev)	Depth of cut (mm)
1	824.6	573.8	818.0	839.0
2	786.3	1024.2	736.2	760.0
3	882.8	895.7	939.4	894.7
Delta	96.4	450.4	203.2	137.4
Rank	4	1	2	3

Table 5: Response table for signal to noise ratios (MRR).

Level	Nanoparticle reinforcement (%)	Spindle speed (rpm)	Machining speed (mm/rev)	Depth of cut (mm)
1	56.60	53.99	56.60	57.35
2	56.42	59.67	56.49	56.06
3	58.03	57.39	57.97	57.66
Delta	1.61	5.68	1.48	1.60
Rank	4	1	2	3

Tables 4 and 5 present the response table for means and response table for S/N ratio, respectively. In these tables, the spindle speed was a higher influence factor of this investigation comparing to others [41]. From the rank order, the factor influence was stated as second rank of machining speed, third rank of depth of cut, and fourth rank is hybrid nanoparticle reinforcement percentage. In the MRR investigation, the optimal factors were obtained as 12% of hybrid nanoparticle reinforcement, 1000 rpm of spindle speed, 0.15 mm/rev, and 1 mm of depth of cut.

Figures 4 and 5 illustrate the main effect plot for means and main effect plot for S/N ratio of material removal rate. Increasing of hybrid nanoparticle reinforcement percentage changes the material removal rate, minimum spindle speed offered low MRR. Moderate level of spindle speed such as 1000 rpm offered higher MRR. Initially, the machining speed 0.05 mm/rev produced good level of MRR, further increasing of feed 0.05 to 0.10 mm/rev the MRR rate was reduced slightly. Feed of 0.15 mm/rev recorded as higher MRR. In depth of cut analysis, 0.75 mm of depth of cut registered as a low level of MRR, and higher MRR was obtained by using of 1.00 mm of depth of cut [42].

From the probability analysis, maximum points lie on the mean line or probability line few points only slightly deviated from the mean line as shown in Figure 6. These points were represented that the chosen parameters, and its correlation was excellent one and also produced better MRR. All the points were scattered homogeneously between the upper and lower limits as shown in Figure 7. Scattered points were positioned within the limits; it has to be enlightened about the relations between the parameters and the accurate results such as MRR.

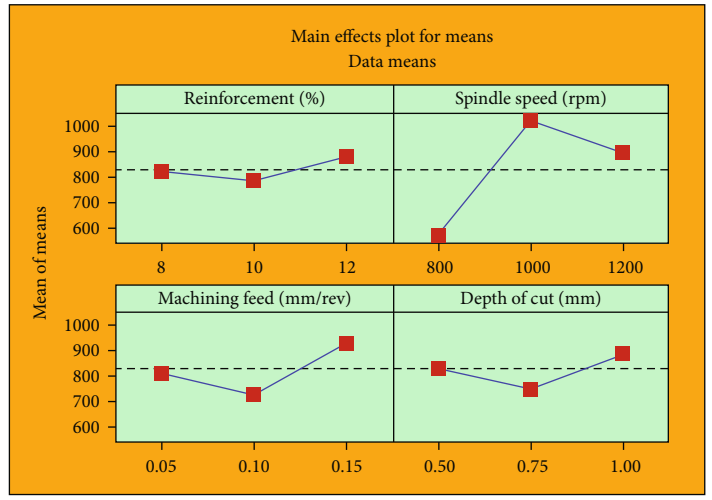

Figure 4: Main effect plot for means (MRR).

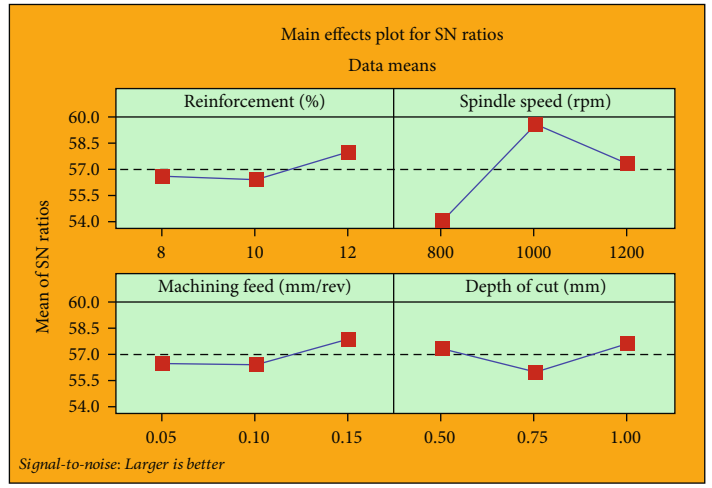

Figure 5: Main effect plot for S/N ratio (MRR).

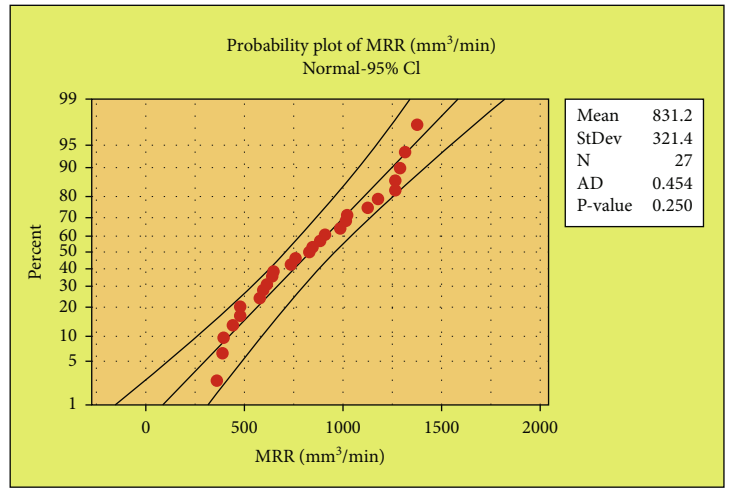

Figure 6: Probability plot of material removal rate.

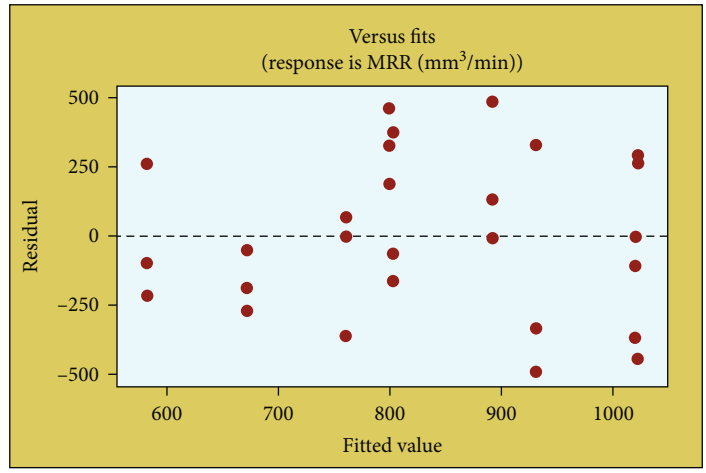

Figure 7: Versus fits plot of material removal rate.

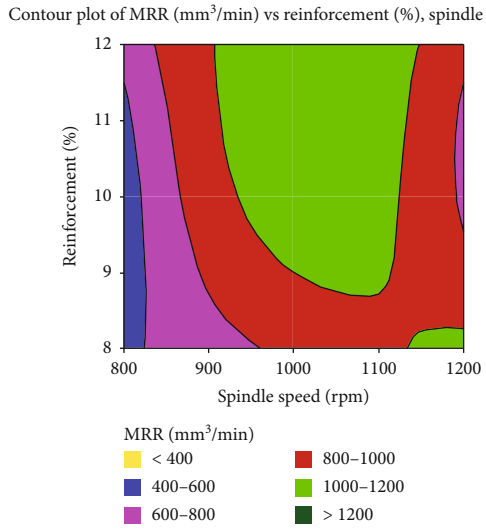

Figure 8: Contour plot: spindle speed vs. reinforcement % for MRR response.

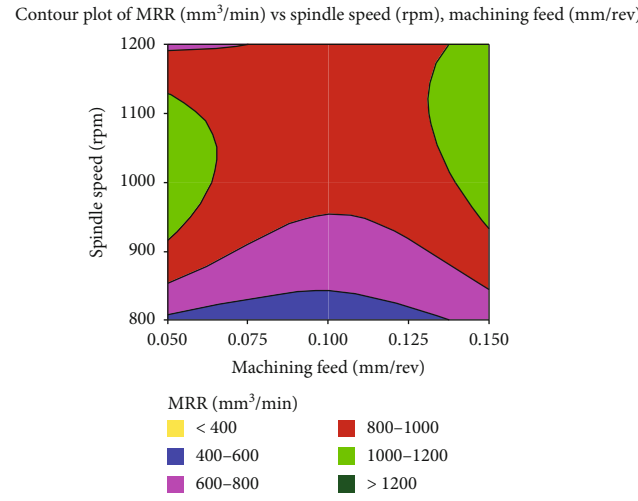

Figure 9: Contour plot: machining feed vs. spindle speed for MRR response.

Figure 8 illustrates that the contour plot of spindle speed and percentage of reinforcement of hybrid nanoparticles, the moderate spindle speed and increasing of percentage of reinforcement of hybrid nanoparticles offered excellent MRR. Above 1000 mm^3/min of MRR was recorded by influencing 1100 rpm of spindle speed and more than 10% of nanoparticle reinforcement. Figure 9 exemplifies the contour plot of machining feed and spindle speed, higher machining speed such as 0.150 mm/rev and moderate spindle speed provided higher MRR. Figure 10 demonstrates that the contour plot of depth of cut and machining speed, the lower value of depth of cut and higher value of machining speed offered maximum of MRR. Contrary minimum machining feed and higher depth of cut offered excellent MRR. Figure 11 represents the contour plot of reinforcement and depth of cut, moderate reinforcement and low level of depth of cut provided enhanced MRR.

Figure 12 shows the pie charts of material removal rate (MRR); this plot enlightens the all-parameter contribution and the outcome (MRR) of the research work individually.

The mathematical model developed to predict the MRR with respect to the nanoparticle reinforcement contribution and machining parameters for the specific requirements and shown in

$$\begin{aligned}\mathrm{MRR}\left(\mathrm{mm}^3/\mathrm{min}\right) &= 831.2 - 6.7 \cdot \mathrm{NS}(\%)\_8 - 44.9 \cdot \mathrm{NS}(\%)\_10 \\ &\quad + 51.6 \cdot \mathrm{NS}(\%)\_12 - 257.4 \cdot \mathrm{SS}(\mathrm{rpm})\_800 \\ &\quad + 193.0 \cdot \mathrm{SS}(\mathrm{rpm})\_1000 + 64.4 \cdot \mathrm{SS}(\mathrm{rpm})\_1200 \\ &\quad - 13.2 \cdot \mathrm{MS}(\mathrm{mm/rev})\_0.05 - 95.0 \cdot \mathrm{MS}(\mathrm{mm/rev})\_0.10 \\ &\quad + 108.2 \cdot \mathrm{MS}(\mathrm{mm/rev})\_0.15 + 7.8\mathrm{DC}(\mathrm{mm})\_0.50 \\ &\quad - 71.2 \cdot \mathrm{DC}(\mathrm{mm})\_0.75 + 63.4 \cdot \mathrm{DC}(\mathrm{mm})\_1.00. \end{aligned} \quad (1)$$

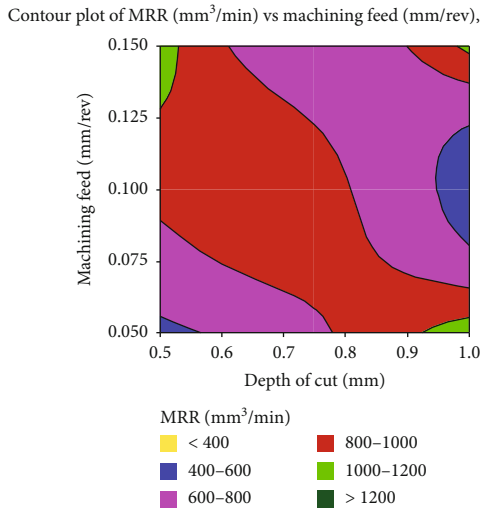

Figure 10: Contour plot: depth of cut vs. machining feed for MRR response.

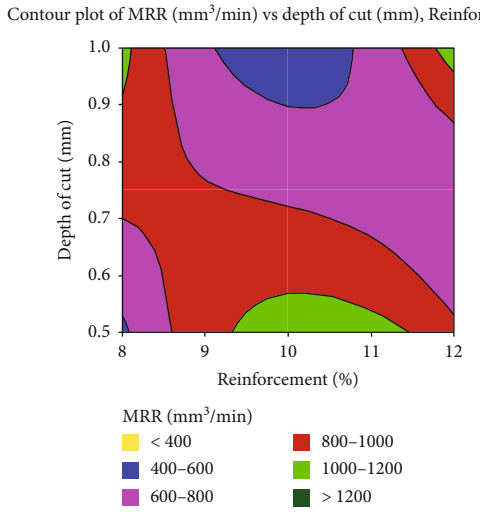

Figure 11: Contour plot: reinforcement % vs. depth of cut for MRR response of nanoparticles.

3.2. Surface Roughness. Table 6 illustrates each parameter relationship and the yield result of surface roughness in elaborate manner. Minimum surface roughness was found as 0.62 μm in the fourth experimental runs. Reduced surface roughness value was obtained by 8% of hybrid nanoparticle reinforcement, 1000 rpm of spindle speed, 0.10 mm/rev of machining speed, and 0.75 mm of depth of cut.

Tables 7 and 8 offer the response table for means and response table for S/N ratio of surface roughness, respectively. In surface roughness analysis, the machining speed was the major influencing factor compared to remaining factors. From the rank order, the machining feed was first, spindle speed was second, hybrid nanoparticle reinforcement percentage was third, and depth of cut was fourth order. Surface roughness analysis provided optimal parameters such as 12% of hybrid nanoparticle reinforcement, 800 rpm of spindle speed, 0.10 mm/rev, and 0.50 mm of depth of cut.

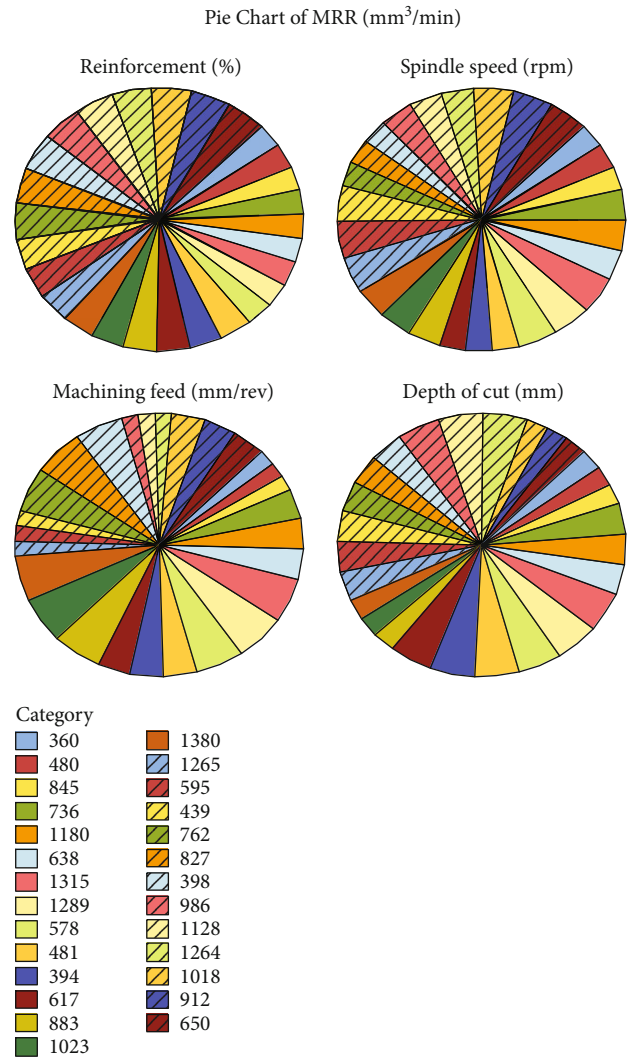

Figure 12: Pie chart of MRR.

Figures 13 and 14 show the main effect plot for means and main effect plot for S/N ratio of surface roughness. Higher hybrid nanoparticle reinforcement percentage (12%) offered minimum surface roughness. Minimum spindle speed such as 800 rpm provided better surface roughness, further increasing spindle speed from 800 rpm to 1200 rpm the surface roughness was showed highly on the surfaces of the specimens. Moderate machining speed such as 0.10 mm/rev offered minimum surface roughness, continually increasing the machining speed 0.15 mm/rev maximum surface roughness was observed. From depth of cut analysis, minimum depth of cut (0.50 mm) produced low surface roughness. Increasing of depth of cut increases the surface roughness values.

In the probability investigation, most of the points touch the mean line; few of them deviated from the mean line as shown in Figure 15. All points close and that touch the mean line represented the correlation among chosen parameters. This analysis proved the selected parameters were accurate ones and make a better surface finish. All the experimental runs were converted into scattered plot; the points were

Table 6: Summary of machining parameters and surface roughness.

Exp. runs	Nanoparticle reinforcement (%)	Spindle speed (rpm)	Machining feed (mm/rev)	Depth of cut (mm)	Surface roughness (μm)
1	8	800	0.05	0.50	0.89
2	8	800	0.05	0.50	1.56
3	8	800	0.05	0.50	1.97
4	8	1000	0.10	0.75	0.62
5	8	1000	0.10	0.75	1.51
6	8	1000	0.10	0.75	1.76
7	8	1200	0.15	1.00	2.01
8	8	1200	0.15	1.00	1.93
9	8	1200	0.15	1.00	1.28
10	10	800	0.10	1.00	0.93
11	10	800	0.10	1.00	0.74
12	10	800	0.10	1.00	0.73
13	10	1000	0.15	0.50	0.83
14	10	1000	0.15	0.50	1.37
15	10	1000	0.15	0.50	1.65
16	10	1200	0.05	0.75	1.47
17	10	1200	0.05	0.75	2.34
18	10	1200	0.05	0.75	1.94
19	12	800	0.15	0.75	0.78
20	12	800	0.15	0.75	0.62
21	12	800	0.15	0.75	1.36
22	12	1000	0.05	1.00	1.82
23	12	1000	0.05	1.00	1.09
24	12	1000	0.05	1.00	1.72
25	12	1200	0.10	0.50	0.94
26	12	1200	0.10	0.50	0.68
27	12	1200	0.10	0.50	1.59

Table 7: Response table for means (surface roughness).

Level	Nanoparticle reinforcement (%)	Spindle speed (rpm)	Machining speed (mm/rev)	Depth of cut (mm)
1	1.503	1.064	1.644	1.276
2	1.333	1.374	1.056	1.378
3	1.178	1.576	1.314	1.361
Delta	0.326	0.511	0.589	0.102
Rank	3	2	1	4

Table 8: Response table for signal to noise ratios (surface roughness).

Level	Nanoparticle reinforcement (%)	Spindle speed (rpm)	Machining speed (mm/rev)	Depth of cut (mm)
1	-3.8472	-0.5433	-4.4996	-2.4393
2	-2.1262	-0.0840	-0.6880	-2.7994
3	-1.6106	-3.9567	-2.3964	-2.3453
Delta	2.2367	3.4134	3.8116	0.4540
Rank	3	2	1	4

scattered homogeneously among the upper and lower limits as shown in Figure 16. Scattered points informed that the points are positioned in correct manner; hence, the parameter relation has enlightened the surface roughness.

Figure 17 demonstrates that the contour plot of spindle speed and hybrid nanoparticle reinforcement percentage, the minimum spindle speed (800 rpm) increasing hybrid nanoparticle reinforcement percentage offered minimum surface roughness. Higher spindle speed affects the surface roughness. Figure 18 illustrates the contour plot of machining feed and spindle speed, increasing machining speed from 0.050 mm/rev and minimum spindle speed presented excellent surface finish. Figure 19 demonstrates the contour plot of depth of cut and machining speed, the higher value of depth of cut and moderate value of machining speed presented minimum surface roughness. Contrary moderate depth of cut and minimum machining feed was increasing the surface roughness. Figure 20 represents the contour plot of hybrid nanoparticle reinforcement percentage and depth of cut, both moderate hybrid nanoparticle reinforcement percentage and depth of cut recorded minimum surface roughness.

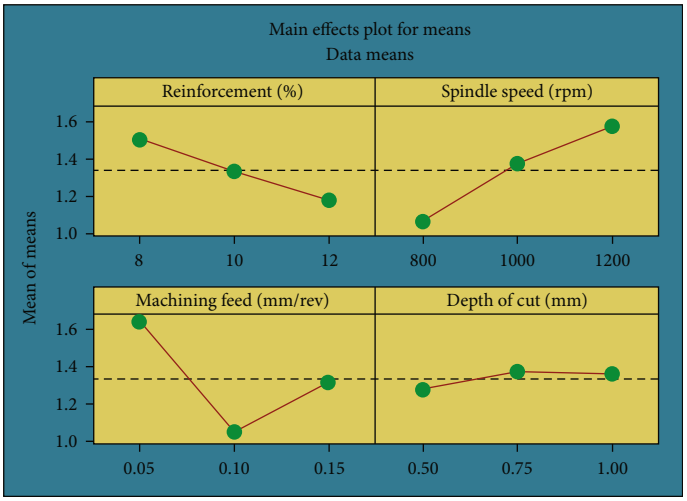

Figure 13: Main effect plot for means (surface roughness).

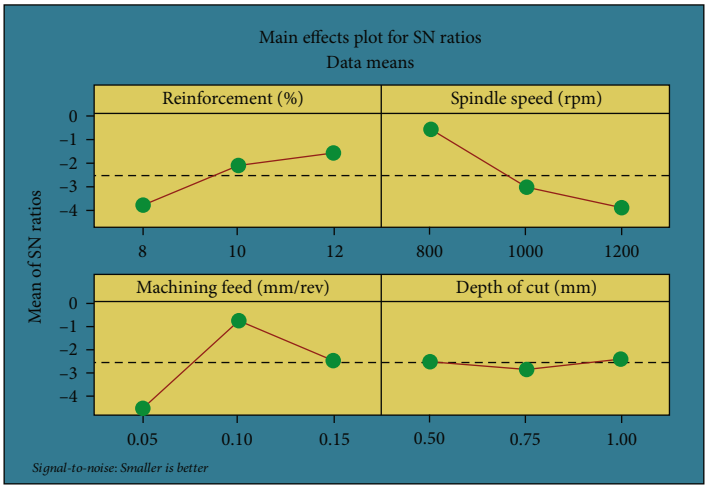

Figure 14: Main effect plot for S/N ratio (surface roughness).

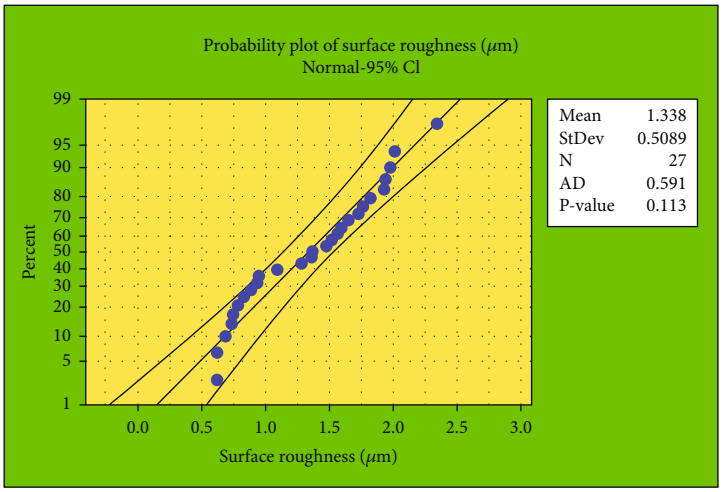

Figure 15: Probability plot of surface roughness.

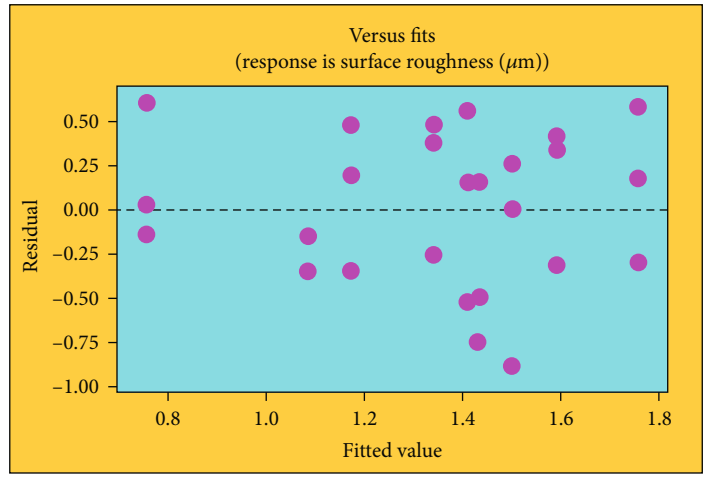

Figure 16: Versus fits plot of surface roughness.

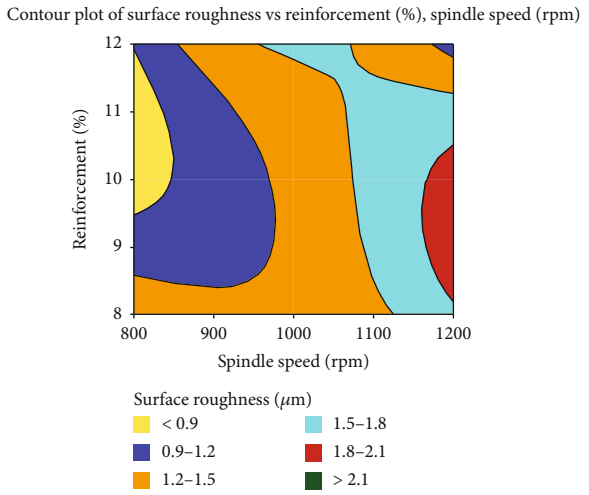

Figure 17: Contour plot: spindle speed vs. nanoparticle reinforcement % for surface roughness response.

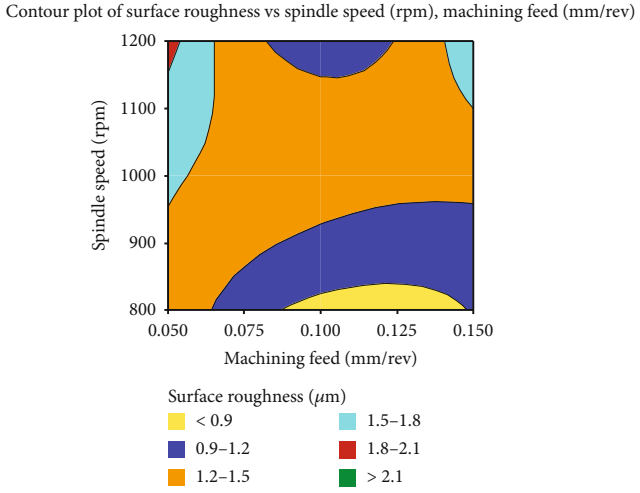

Figure 18: Contour plot: machining feed vs. spindle speed for surface roughness response.

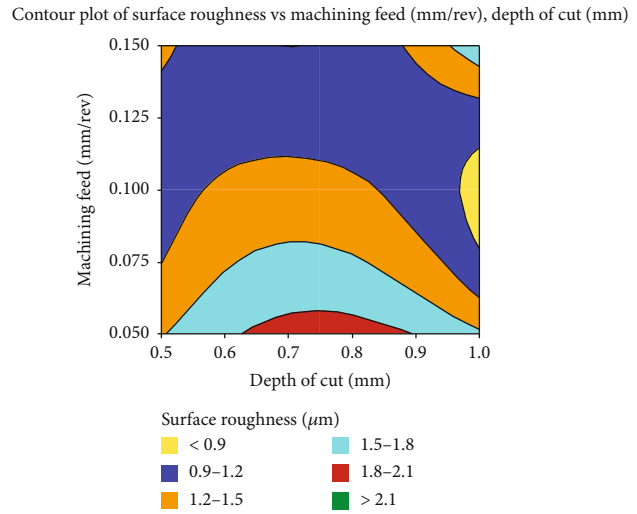

Figure 19: Contour plot: depth of cut vs. machining feed for surface roughness response.

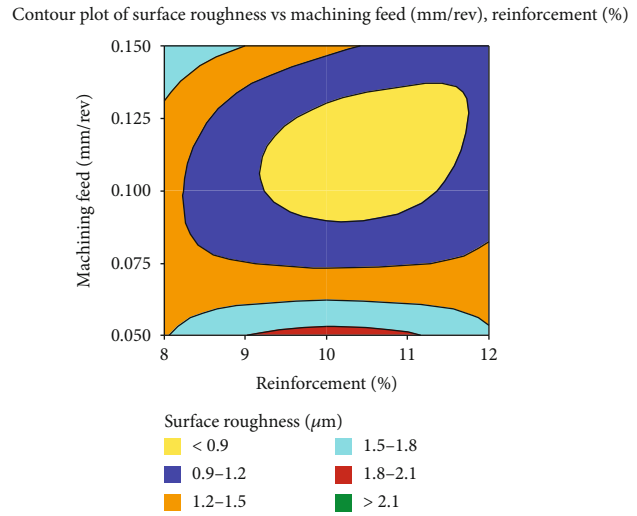

Figure 20: Contour plot: machining feed vs. nanomaterial reinforcement for surface roughness response.

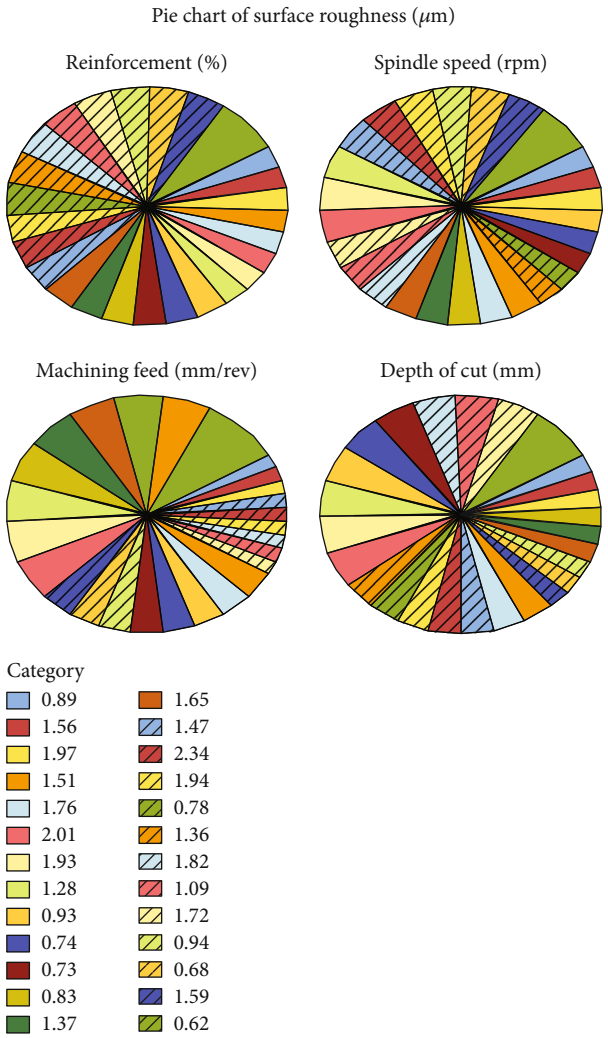

Figure 21: Pie chart of surface roughness.

Figure 21 illustrates the pie charts of surface roughness; this plot makes clear all parameter involvement and the result (surface roughness) of the investigation individually. The mathematical model developed and shown below to predict the surface roughness with respect to the hybrid nanoparticle reinforcement percentage and machining parameters for the specific requirements and shown in

$$\begin{aligned}\text{Surface}\cdot\text{roughness}(\mu\text{m}) &= 1.3381 + 0.165\text{NS}(\%)\_8 - 0.005\text{NS}(\%)\_10 \\ &\quad - 0.160\text{NS}(\%)\_12 - 0.274\text{SS}(\text{rpm})\_800 \\ &\quad + 0.036\text{SS}(\text{rpm})\_1000 + 0.237\text{SS}(\text{rpm})\_1200 \\ &\quad + 0.306\text{MS}(\text{mm/rev})\_0.05 \\ &\quad - 0.283\text{MS}(\text{mm/rev})\_0.10 \\ &\quad - +0.024\text{MS}(\text{mm/rev})\_0.15 - 0.063\text{DC}(\text{mm})\_0.50 \\ &\quad + 0.040\text{DC}(\text{mm})\_0.75 + 0.023\text{DC}(\text{mm})\_1.00.\end{aligned} \quad (2)$$

It was observed that machinability condition requirements vary for each grade (based on hybrid nanoparticle reinforcement percentage) of novel AMMC of AA8050/B_4C/TiB_2. The developed mathematical model will support to make right choice in manufacturing and machining.

4. Conclusion

This research work was carried out for CNC turning with different process parameters that influence to obtain enhanced MRR and surface roughness of hybrid AMMC's (AA8050/B_4C/TiB_2) successfully. Diamond-Like Carbon-(DLC-) coated tungsten carbide tool was used to conduct the turning process with chosen parameters. The results were concluded as follows:

(i) From the MRR analysis, maximum material removal rate of 1380 mm^3/min was obtained by 10% hybrid nanoparticle reinforcement, 1000 rpm of spindle speed, 0.15 mm/rev of machining speed, and 0.50 mm of depth of cut. In the MRR investigation, the optimal factors were registered as 12% hybrid nanoparticle reinforcement, 1000 rpm of spindle speed, 0.15 mm/rev, and 1 mm of depth of cut

(ii) Moderate level of spindle speed such as 1000 rpm offered higher MRR. Initially, the machining speed 0.05 mm/rev produced good level of MRR, further increasing of feed 0.05 to 0.10 mm/rev the MRR rate was reduced slightly

(iii) In the surface roughness investigations, minimum surface roughness was found as 0.62 μm in the fourth experimental runs. Reduced surface roughness value was obtained by 8% hybrid nanoparticle reinforcement, 1000 rpm of spindle speed, 0.10 mm/rev of machining speed, and 0.75 mm of depth of cut. Surface roughness analysis provided optimal parameters such as 12% hybrid nanoparticle reinforcement, 800 rpm of spindle speed, 0.10 mm/rev, and 0.50 mm of depth of cut

(iv) From the depth of cut analysis, minimum depth of cut (0.50 mm) formed low surface roughness. Increasing of depth of cut increases the surface roughness values

As aluminium alloys are widely utilized for numerous applications and selection of materials done for the application specific from the range of desired mechanical properties, this novel AMMC type of altering existing mechanical properties like enhanced wear resistance, self-lubrication properties for an automobile spare manufacturing application and this work developed mathematical models for process planning for manufacturing and machining. Hence, this piece of research claims a high social implication.

Data Availability

The data used to support the findings of this study are included within the article. Further data or information is available from the corresponding author upon request.

Conflicts of Interest

The authors declare that there is no conflict of interest regarding the publication of this article.

Acknowledgments

The authors appreciate the supports from Haramaya University, Ethiopia, for providing help during the research and preparation of the manuscript. The authors thank Saveetha School of Engineering, Vel Tech Rangarajan Dr. Sagunthala R&D Institute of Science and Technology, for providing assistance to this work. The authors would like to acknowledge the Researchers Supporting Project number (RSP-2021/373), King Saud University, Riyadh, Saudi Arabia.

References

[1] R. A. Laghari, J. Li, and M. Mia, "Effects of turning parameters and parametric optimization of the cutting forces in machining SiCp/Al 45 wt% composite," *Metals*, vol. 10, no. 6, p. 840, 2020.

[2] B. R. Krishnan and M. Ramesh, "Optimization of machining process parameters in CNC turning process of IS2062 E250 Steel using coated carbide cutting tool," *Materials Today: Proceedings*, vol. 21, pp. 346–350, 2020.

[3] N. Senthilkumar, T. Ganapathy, and T. Tamizharasan, "Optimisation of machining and geometrical parameters in turning process using Taguchi method," *Australian Journal of Mechanical Engineering*, vol. 12, no. 2, pp. 233–246, 2014.

[4] N. Szczotkarz, R. Mrugalski, R. W. Maruda et al., "Cutting tool wear in turning 316L stainless steel in the conditions of minimized lubrication," *Tribology International*, vol. 156, p. 106813, 2021.

[5] C. Agrawal, N. Khanna, C. I. Pruncu, A. K. Singla, and M. K. Gupta, "Tool wear progression and its effects on energy consumption and surface roughness in cryogenic assisted turning of Ti-6Al-4V," *The International Journal of Advanced Manufacturing Technology*, vol. 111, no. 5, pp. 1319–1331, 2020.

[6] A. Kannan, R. Mohan, R. Viswanathan, and N. Sivashankar, "Experimental investigation on surface roughness, tool wear and cutting force in turning of hybrid (Al7075+ SiC+ Gr) metal matrix composites," *Journal of Materials Research and Technology*, vol. 9, no. 6, pp. 16529–16540, 2020.

[7] K. Balasubramanian, M. Nataraj, and D. Palanisamy, "Machinability analysis and application of response surface approach on CNC turning of LM6/SiCp composites," *Materials and Manufacturing Processes*, vol. 34, no. 12, pp. 1389–1400, 2019.

[8] S. A. Niknam, S. Kamalizadeh, A. Asgari, and M. Balazinski, "Turning titanium metal matrix composites (MMCs) with carbide and CBN inserts," *The International Journal of Advanced Manufacturing Technology*, vol. 97, no. 1-4, pp. 253–265, 2018.

[9] M. Kuntoğlu and H. Sağlam, "Investigation of progressive tool wear for determining of optimized machining parameters in turning," *Measurement*, vol. 140, pp. 427–436, 2019.

[10] J. Allen Jeffrey, S. Suresh Kumar, P. Vaidyaa, A. Nicho, A. Chrish, and J. Joshith, "Effect of turning parameters in cylindricity and circularity for o1 steel using ANN," *Materials Today: Proceedings*, vol. 59, no. 2, pp. 1291–1294, 2022.

[11] N. Kawin, D. Jagadeesh, G. Saravanan, and K. Periasamy, "Optimization of turning parameters in sugarcane bagasse ash reinforced with Al-Si10-Mg alloy composites by Taguchi method," *Materials Today: Proceedings*, vol. 21, pp. 474–476, 2020.

[12] M. Mia, P. R. Dey, M. S. Hossain et al., "Taguchi S/N based optimization of machining parameters for surface roughness, tool wear and material removal rate in hard turning under MQL cutting condition," *Measurement*, vol. 122, pp. 380–391, 2018.

[13] N. G. S. Kumar, G. S. Shiva Shankar, M. N. Ganesh, and L. K. Vibudha, "Experimental investigations to study the cutting force and surface roughness during turning of aluminium metal matrix hybrid composites," *Materials Today: Proceedings*, vol. 4, no. 9, pp. 9371–9374, 2017.

[14] S. K. Shihab, Z. A. Khan, and A. N. Siddiquee, "RSM based investigations on the effects of cutting parameters on surface integrity during cryogenic hard turning of AISI 52100," *Journal for Manufacturing Science and Production*, vol. 15, no. 3, pp. 309–318, 2015.

[15] Y. Xiong, W. Wang, R. Jiang, K. Lin, and G. Song, "Surface integrity of milling in-situ TiB2 particle reinforced Al matrix composites," *International Journal of Refractory Metals and Hard Materials*, vol. 54, pp. 407–416, 2016.

[16] M. M. Ravikumar, S. Suresh Kumar, R. Vishnu Kumar, S. Nandakumar, J. Habeeb Rahman, and J. Ashok Raj, "Evaluation on mechanical behavior of AA2219/SiO_2 composites made by stir casting process," *AIP Conference Proceedings*, vol. 2405, article 50010, 2022.

[17] Z. Liao, A. Abdelhafeez, H. Li, Y. Yang, O. G. Diaz, and D. Axinte, "State-of-the-art of surface integrity in machining of metal matrix composites," *International Journal of Machine Tools and Manufacture*, vol. 143, pp. 63–91, 2019.

[18] R. K. Thakur, D. Sharma, and K. K. Singh, "Optimization of surface roughness and delamination factor in end milling of graphene modified GFRP using response surface methodology," *Materials Today: Proceedings*, vol. 19, pp. 133–139, 2019.

[19] J. Li, X. Yang, C. Ren, G. Chen, and Y. Wang, "Multiobjective optimization of cutting parameters in Ti-6Al-4V milling process using nondominated sorting genetic algorithm-II," *The International Journal of Advanced Manufacturing Technology*, vol. 76, no. 5-8, pp. 941–953, 2015.

[20] T.-S. Lan, K.-C. Chuang, and Y.-M. Chen, "Optimization of machining parameters using fuzzy Taguchi method for reducing tool wear," *Applied Sciences*, vol. 8, no. 7, p. 1011, 2018.

[21] V. Parashar and R. Purohit, "Analysis of machining behavior of Al/A206-Al2O3 metal matrix composite using end milling process," *Materials Today: Proceedings*, vol. 4, no. 2, pp. 2687–2692, 2017.

[22] R. Sridhar, S. P. Subramaniyan, and S. Ramesh, "Optimization of machining and geometrical parameters to reduce vibration while milling metal matrix composite," *Transactions of the Indian Institute of Metals*, vol. 72, no. 12, pp. 3179–3189, 2019.

[23] P. S. Bains, S. S. Sidhu, and H. S. Payal, "Fabrication and machining of metal matrix composites: a review," *Materials and Manufacturing Processes*, vol. 31, no. 5, pp. 553–573, 2016.

[24] A. I. Jumare, K. Abou-El-Hossein, L. N. Abdulkadir, and M. M. Liman, "Predictive modeling and multiobjective

optimization of diamond turning process of single-crystal silicon using RSM and desirability function approach," *The International Journal of Advanced Manufacturing Technology*, vol. 103, no. 9, pp. 4205–4220, 2019.

[25] R. Butola, C. Pratap, A. Shukla, and R. S. Walia, "Effect on the mechanical properties of aluminum-based hybrid metal matrix composite using stir casting method," *In Materials Science Forum[Trans Tech Publications Ltd]*, vol. 969, pp. 253–259, 2019.

[26] V. Gaikhe, J. Sahu, and R. Pawade, "Optimization of cutting parameters for cutting force minimization in helical ball end milling of Inconel 718 by using genetic algorithm," *Procedia CIRP*, vol. 77, pp. 477–480, 2018.

[27] S. Daniel, R. Ajith Arul, and R. Pugazhenthi, "Multi objective prediction and optimization of control parameters in the milling of aluminium hybrid metal matrix composites using ANN and Taguchi -grey relational analysis," *Technology*, vol. 15, no. 4, pp. 545–556, 2019.

[28] H. Tebassi, M. Yallese, R. Khettabi, S. Belhadi, I. Meddour, and F. Girardin, "Multi-objective optimization of surface roughness, cutting forces, productivity and Power consumption when turning of Inconel 718," *International Journal of Industrial Engineering Computations*, vol. 7, no. 1, pp. 111–134, 2016.

[29] M. Nataraj and K. Balasubramanian, "Parametric optimization of CNC turning process for hybrid metal matrix composite," *The International Journal of Advanced Manufacturing Technology*, vol. 93, no. 1-4, pp. 215–224, 2017.

[30] R. Butola, S. Kanwar, L. Tyagi, R. M. Singari, and M. Tyagi, "Optimizing the machining variables in CNC turning of aluminum based hybrid metal matrix composites," *SN Applied Sciences*, vol. 2, no. 8, pp. 1–9, 2020.

[31] W. Bai, A. Roy, R. Sun, and V. V. Silberschmidt, "Enhanced machinability of SiC-reinforced metal-matrix composite with hybrid turning," *Journal of Materials Processing Technology*, vol. 268, pp. 149–161, 2019.

[32] T. Sathish, N. Sabarirajan, and S. Karthick, "Machining parameters optimization of aluminium alloy 6063 with reinforcement of SiC composites," *Materials Today: Proceedings*, vol. 33, pp. 2559–2563, 2020.

[33] R. Das, S. S. Mohanty, M. Panigrahi, and S. Mohanty, "Predictive modelling and analysis of surface roughness in CNC milling of green alumina using response surface method and genetic algorithm," in *1st International Conference on Advanced Engineering Functional Materials (ICAEFM) 21–23 September 2018, GITA [vol. 410, no. 1]*, In IOP Conference Series: Materials Science and Engineering, p. 12022, IOP Publishing, Bhubaneswar, Odisha, India, 2018.

[34] Ş. Karabulut, U. Gökmen, and H. Çinici, "Optimization of machining conditions for surface quality in milling AA7039-based metal matrix composites," *Arabian Journal for Science and Engineering*, vol. 43, no. 3, pp. 1071–1082, 2018.

[35] T. Sathish and N. Sabarirajan, "Synthesis and optimization of AA 7175-zirconium carbide composites machining parameters," *Journal of New Materials for Electrochemical systems*, vol. 24, pp. 34-3–3417, 2021.

[36] J. Pfrommer, C. Zimmerling, J. Liu, L. Kärger, F. Henning, and J. Beyerer, "Optimisation of manufacturing process parameters using deep neural networks as surrogate models," *Procedia CiRP*, vol. 72, pp. 426–431, 2018.

[37] T. Ding, S. Zhang, Y. Wang, and X. Zhu, "Empirical models and optimal cutting parameters for cutting forces and surface roughness in hard milling of AISI H13 steel," *The International Journal of Advanced Manufacturing Technology*, vol. 51, no. 1-4, pp. 45–55, 2010.

[38] A. R. Shinge and U. A. Dabade, "The effect of process parameters on material removal rate and dimensional variation of channel width in micro-milling of aluminium alloy 6063 T6," *Procedia Manufacturing*, vol. 20, pp. 168–173, 2018.

[39] P. Gao, Z. Liang, X. Wang, S. Li, and T. Zhou, "Effects of different chamfered cutting edges of micro end mill on cutting performance," *International Journal of Advanced Manufacturing Technology*, vol. 96, no. 1-4, pp. 1215–1224, 2018.

[40] B. Das, S. Roy, R. N. Rai, and S. C. Saha, "Application of grey fuzzy logic for the optimization of CNC milling parameters for Al–4.5% Cu–TiC MMCs with multi-performance characteristics," *Engineering Science and Technology, an International Journal*, vol. 19, no. 2, pp. 857–865, 2016.

[41] O. Aguş, Y. Abalı, O. Arslan, and N. O. S. Keskin, "Facile and controlled production of silver borate nanoparticles," *SN Applied Sciences*, vol. 1, no. 7, pp. 1–8, 2019.

[42] M. Pul, "The effect of MgO ratio on surface roughness in Al-MgO composıtes," *Materials and Manufacturing Processes*, vol. 28, no. 9, pp. 963–968, 2013.